



## STRUCTURAL AND ELECTRONIC PROPERTIES OF SULFUR PASSIVATED InP(100)

C. E. J. Mitchell\*, I. G. Hill\*, A. B. McLean\*  
and Z. H. Lu†

\*Department of Physics, Queen's University, Kingston,  
Canada K7L 3N6

†Institute for Microstructural Sciences, National Research Council of  
Canada, Ottawa, Canada K1A 0R6

### Abstract

InP(100) surfaces were passivated with S using a wet chemical treatment. The structural properties of the passivated surface were studied with low-energy electron diffraction. In agreement with previous studies, a  $1 \times 1$  pattern was observed for the as-passivated surface, while a  $2 \times 1$  reconstruction was found for surfaces annealed at temperatures in the range  $350^\circ\text{C} - 500^\circ\text{C}$ . Photoemission and inverse photoemission were used to examine the electronic properties of the surface. The sulfur treatment was found to remove both occupied and unoccupied states from the vicinity of the fundamental gap. The surface bandgap at the zone centre,  $\bar{\Gamma}$ , on the passivated surface was measured to be 5.1 eV, as compared to 2.5 eV for the clean, sputter/annealed  $2 \times 4$  surface. No partially filled bands were observed crossing the Fermi level.

### Abbreviations

AES	Auger Electron Spectroscopy
LEED	Low-Energy Electron Diffraction
MISFET	Metal-Insulator-Semiconductor Field Effect Transistor
ML	Monolayer
RHEED	Reflection High-Energy Electron Diffraction
UHV	Ultra High Vacuum
XANES	X-ray Absorption Near Edge Spectroscopy
XPD	X-ray Photoelectron Diffraction
XPS	X-ray Photoelectron Spectroscopy

## 1. Introduction

Although the bulk electronic properties of InP make it an ideal choice for many devices, such as MISFETS [1, 2], it is difficult to terminate the (100), the most common growth surface, with a high quality layer which is electrically passive. The native oxide is of poor quality and the interface between the semiconductor and the oxide contains a high density of defects which act as recombination centres. These interfacial traps give rise to a large recombination contribution to the I-V characteristics of MIS diodes fabricated on InP(100) and they also cause substantial dispersion in the C-V characteristics [1, 3]. To surmount these problems, several methods have been developed to passivate InP(100). At the present time, the most promising appears to be a wet chemical treatment with  $(\text{NH}_4)_2\text{S}$ . This has been shown to substantially reduce the density of recombination centres in MIS diodes [1]. Consequently, it is possible that this simple process could be used to improve the quality of practical devices.

From a fundamental point of view, there is much to be learned about the passivation process. Although there has been a significant amount of experimental work already devoted to studying the structure and properties of S-passivated InP(100), it is still unclear why the addition of S passivates the InP(100) surface. Both  $1 \times 1$  [4] and  $2 \times 1$  [5, 6] patterns have been observed with low-energy electron diffraction (LEED) and reflection high-energy electron diffraction (RHEED). X-ray photoelectron spectroscopy (XPS) results [4, 5, 7] as well as an x-ray absorption near-edge spectroscopy (XANES) study [8] indicate that S is bonded to In, and that the surface S occupies bridge positions. XPS and X-ray photoelectron diffraction (XPD) experiments [5, 7] provide evidence for the presence of subsurface sulfur. The sulfur coverage has been found to be approximately 1 ML [4, 5, 6]. In this paper, we use low-energy electron diffraction, photoemission and inverse photoemission to investigate the electronic and atomic structure of the surface.

## 2. Experimental

The experiments were performed in an ultra high vacuum (UHV) chamber which has a base pressure of  $8 \times 10^{-11}$  Torr. All photoemission and inverse photoemission measurements are angle-resolved. The photoemission experiments were performed with a differentially pumped resonance lamp and a hemispherical electron energy analyser with a 50mm mean radius. The inverse photoemission experiments were performed with a home-built electron gun [9] and a bandpass photon detector consisting of a  $\text{CaF}_2$  window and a Cu-Be electron multiplier [10, 11]. The photoemission and inverse photoemission energy scales can be aligned by using the hemispherical analyser to measure the kinetic energy of electrons produced by the electron gun [12]. This allows us to accurately measure gaps between occupied and unoccupied states without resorting to a secondary reference. The low-energy electron diffraction studies were performed using a Princeton Research Instruments RVL 8-120 reverse view LEED system. The samples were mounted on Mo sample holders and transferred from atmosphere into UHV through a custom load lock system which is evacuated using a turbomolecular pump.

Epiready n-type InP(100) wafers (Crystacom), both unintentionally doped with a carrier

density of  $5.6 \times 10^{15} \text{ cm}^{-3}$  and Sn doped with a carrier density of  $1.2 \times 10^{18} \text{ cm}^{-3}$ , were used in the experiments. The wafers were immersed in ammonium sulfide solution (20.1%  $(\text{NH}_4)_2\text{S}$ ) for 15 min. at a temperature of  $65^\circ\text{C}$ . They were then dipped in ammonium sulfide solution (20.1%  $(\text{NH}_4)_2\text{S}$ ) at room temperature and blown dry with Ar. Sample mounting was also performed while blowing Ar over the sample. The samples were transferred directly into UHV and annealed at  $350^\circ\text{C}$  in order to remove physisorbed gases and to order the overlayers. The principal gases found to be desorbing from the samples were  $\text{H}_2\text{O}$ ,  $\text{SO}_2$ , and  $\text{NH}_3$ . The samples were brought up to the annealing temperature slowly and left at that temperature for 5-10 min. No differences were observed in the results for the unintentionally n doped and Sn doped samples.

The photoemission results reported here were obtained after annealing at  $350^\circ\text{C}$  as described above. LEED studies were performed as a function of annealing temperature. In each case the sample was annealed at the specified temperature for approximately ten minutes. The sample was allowed to cool to room temperature before taking the LEED data.

Photoemission and inverse photoemission studies were also performed on clean InP(100) surfaces. Sn doped (n-type, carrier density  $1.2 \times 10^{18} \text{ cm}^{-3}$ ) epitaxial InP(100) wafers (Crystacomm) were inserted into the vacuum untreated, and cleaned by Ne ion bombardment (20 min. at  $1 \mu\text{A}/\text{cm}^2$ , 500 eV) and subsequent 10 min. anneal at  $350^\circ\text{C}$ .

### 3. Results

A  $1 \times 1$  LEED pattern was obtained from the as-passivated surface. As the sample was annealed to successively higher temperatures, up to  $\approx 350^\circ\text{C}$ , the intensity of the first-order spots increased, while the background intensity diminished. This behaviour is consistent with the desorption and/or ordering of a disordered S layer, as is discussed below. At annealing temperatures in the range  $350^\circ\text{C} - 500^\circ\text{C}$ ,  $\frac{1}{2}$ -order spots were observed in the LEED pattern, along the  $[0\bar{1}1]$  direction. The quality and onset temperature of the  $2 \times 1$  pattern varied from sample to sample, probably due to slight differences in the preparation procedure. In all cases, the  $\frac{1}{2}$ -order spots were broader and less intense than the first-order spots. This is illustrated in Fig. 1, where a line profile taken along the  $[0\bar{1}1]$  direction of the LEED pattern is shown. The width of the  $\frac{1}{2}$ -order spots is consistent with ordered regions approximately 10 unit cells across. In some of the  $2 \times 1$  patterns obtained, the  $\frac{1}{2}$ -order spots are split, indicating the formation of antiphase domains. There is some indication in the asymmetric lineshape of the  $\frac{1}{2}$ -order spots shown in Fig. 1 that these spots are in fact split, but that the splitting is not resolved.

After annealing to  $\approx 500^\circ\text{C}$ , a  $2 \times 4$  LEED pattern was observed, as illustrated in Fig. 2. The  $\frac{1}{4}$ -order spots lie along the  $[011]$  direction, while the  $\frac{1}{2}$ -order spots lie along  $[0\bar{1}1]$ . The appearance and orientation of the LEED pattern is the same as that typically observed on clean, sputter/annealed or thermally treated InP(100) surfaces. The  $2 \times 4$  LEED pattern was accompanied by the presence of macroscopic In droplets on the surface. The appearance of In droplets is expected as the InP(100) surface begins to decompose through the preferential loss of P [2]. The presence of the  $2 \times 4$  pattern after annealing to a temperature near  $500^\circ\text{C}$  is consistent with previous work

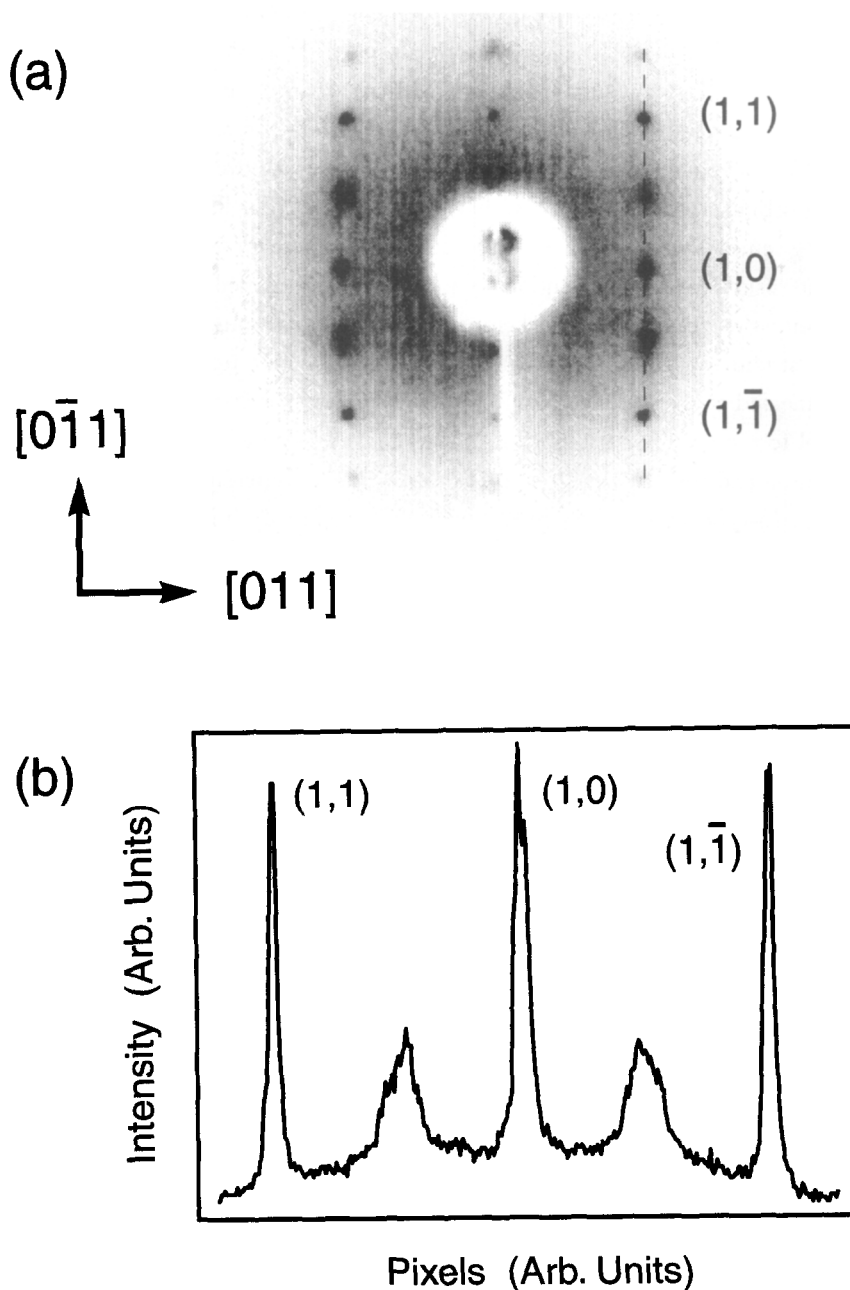


**Fig. 1.** (a) A  $2 \times 1$  LEED pattern obtained on InP(100)-S after annealing to  $450^\circ\text{C}$ . The gun energy is 85 eV. (b) A line profile taken along the  $[0\bar{1}1]$  direction shows the relative width of the  $\frac{1}{2}$ -order spots as compared to the first-order spots.

indicating that the S-terminated surface is stable up to this temperature [6, 13]. One group [5] has reported a stable  $2 \times 1$  reconstruction up to  $560^\circ\text{C}$ . Differences in annealing procedure are a likely explanation for the discrepancy, since the system is expected to be sensitive to annealing time once preferential P desorption starts to occur [2]. We also observed a  $2 \times 4$  pattern on the clean InP(100) surfaces prepared by ion bombardment and annealing to  $350^\circ\text{C}$ .

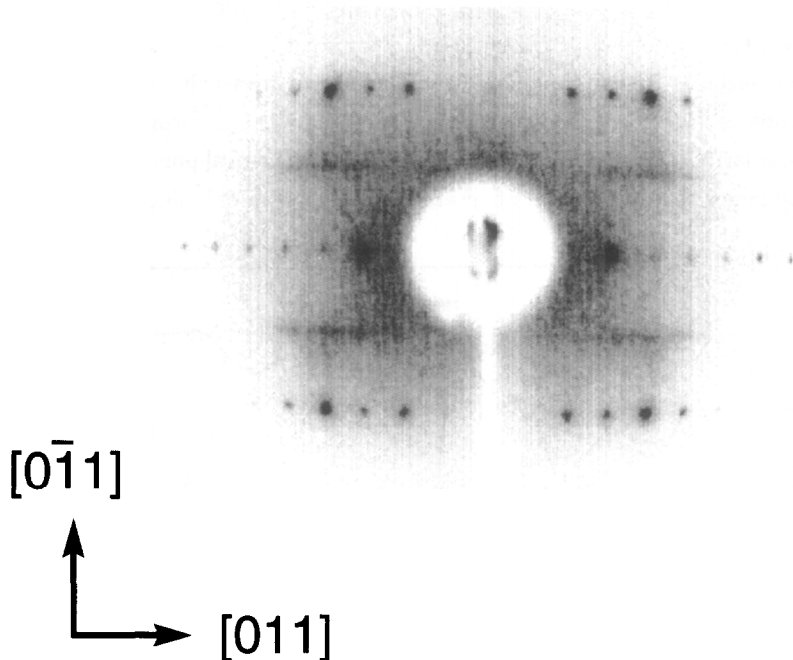


**Fig. 2.** A  $2 \times 4$  LEED pattern obtained after annealing the passivated surface to approximately  $500^\circ\text{C}$ . The gun energy is 75 eV. This LEED pattern was accompanied by the appearance of macroscopic In droplets on the surface.

The surface band bending and the effect of the passivation on surface states in the region of the fundamental gap of InP(100) were investigated with a combination of photoemission and inverse photoemission. In Fig. 3, photoemission and inverse photoemission spectra obtained at the zone centre,  $\bar{\Gamma}$ , are presented for both the clean  $2 \times 4$  and S-passivated  $2 \times 1$  surfaces. The band bending on the clean surface, and the features of the clean surface photoemission spectrum, are consistent with previous work [14, 15]. The valence band features on the S-passivated surface are shifted to higher binding energy. Since the samples investigated were n-type, this indicates a smaller degree of band bending on the S-passivated surface as compared to the clean surface. This result is consistent with the removal of electronic states from the fundamental gap. Two surface features can be seen in the photoemission and inverse photoemission spectra obtained from the clean surface. The sharp peak in the photoemission spectrum at  $\approx 1$  eV below the Fermi level has been assigned by previous authors to P dangling bonds [14]. The feature seen with inverse photoemission at  $\approx 1.5$  eV above the Fermi level is consistent in energy position

with an unoccupied state seen on sputter/annealed GaAs(100)  $4 \times 2$ , which has been assigned to Ga dangling bonds [16] (note that the crystallographic directions given by the authors indicate that their  $4 \times 2$  pattern is equivalent to our  $2 \times 4$  pattern). This feature is therefore tentatively assigned to In dangling bonds. As can be seen from Fig. 3, both of these surface features are removed by the S-passivation.

The surface bandgap at the zone centre,  $\bar{\Gamma}$ , can be determined from the data presented in Fig. 3. As shown, this gap is 2.5 eV for the sputter/annealed  $2 \times 4$  surface, while it is 5.1 eV for the S-passivated surface. It should be noted that we are not measuring the bulk bandgap. Since the photoemission and inverse photoemission experiments were performed at fixed photon energies and not necessarily at an energy where emission from the critical points is observed, the measured gap may be larger than the room temperature bulk bandgap of 1.35 eV [17].

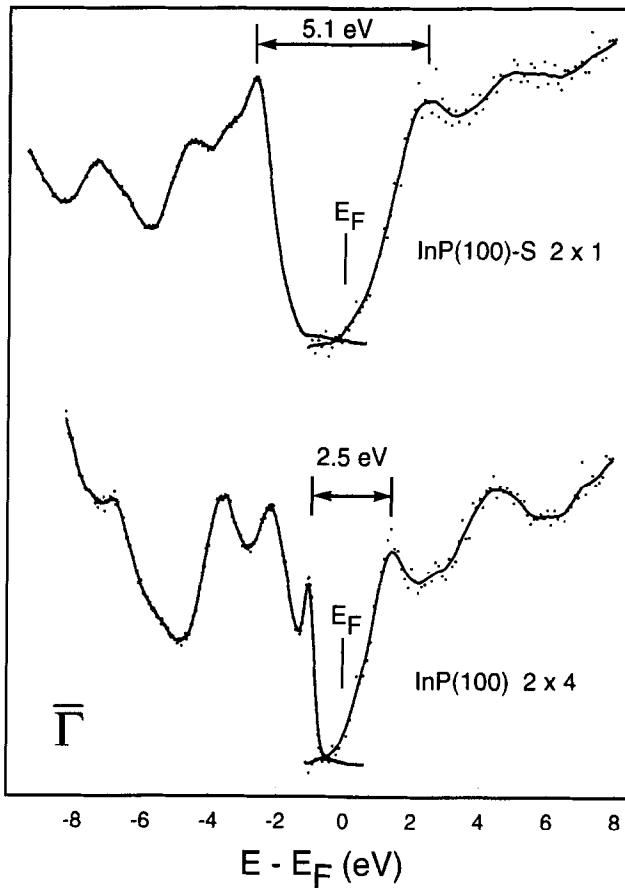


**Fig. 3.** Photoemission and inverse photoemission spectra obtained in normal emission are shown for InP(100)-S  $2 \times 1$  and InP(100)  $2 \times 4$ . The alignment of the spectra is discussed in the text. The Fermi level is marked in the figure, but was not used to align the spectra. The surface bandgap is marked in both cases.

It can further be noted from Fig. 3 that no states are seen near the Fermi level on the S-passivated surface. In addition to the normal emission measurements, photoemission spectra were obtained along both high symmetry lines of the Surface Brillouin Zone ( $\bar{\Gamma}\bar{J}$  and  $\bar{\Gamma}\bar{J}'$ ) on the  $2 \times 1$  and  $1 \times 1$  surfaces. Some representative spectra are shown in Fig. 4. The features marked A, B and C have tentatively been identified as surface-related [18]. Measurements were also performed along the zone edges [19]. No evidence was found for any bands crossing the Fermi level, indicating that there are no partially filled surface bands.

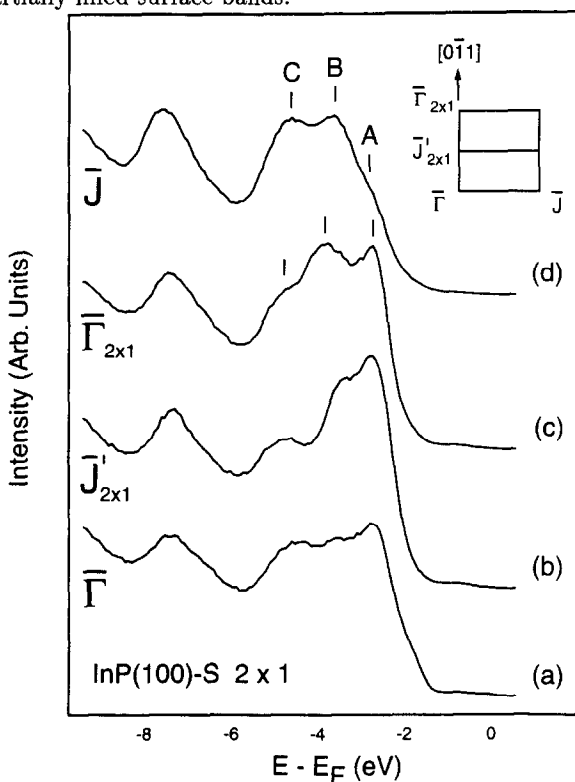


**Fig. 4.** Photoemission obtained on InP(100)-S  $2 \times 1$  is shown for several high symmetry points in the Surface Brillouin Zone. The photon energy is 21.2 eV and the takeoff angles are  $0^\circ$ ,  $12^\circ$  and  $24^\circ$  respectively along  $[0\bar{1}1]$  for (a), (b) and (c). For (d), the takeoff angle is  $24^\circ$  along  $[011]$ . The angles were chosen such that in each case  $k_{||}$  is at the indicated symmetry point for the feature labelled A.

#### 4. Discussion

While sulfur passivation of InP(100) is simple to perform, the changes taking place at the surface during the chemical treatment and subsequent annealing are complex, and it is of interest to formulate a realistic picture of the resulting surface. The immersion of the InP(100) wafer in  $(\text{NH}_4)_2\text{S}$  solution is known to both etch the surface and cover it with sulfur [6]. Recent XPS results obtained by Chassé et.al. [7] on an unannealed  $(\text{NH}_4)_2\text{S}$ -treated surface show the existence of three components in the S2p core level. These components are interpreted as being due to S in subsurface P sites, S bridge-bonded to In at the surface, and a polysulfidic (S-S) species

on the surface. The polysulfidic species is reported to disappear after annealing to 320°C. The transformation that we observed from a weak  $1 \times 1$  diffraction pattern to a much better  $1 \times 1$  pattern with a low background after the sample was annealed to temperatures slightly less than 350°C is consistent with the desorption of a disordered polysulfidic overlayer as implied by the XPS study. While the treatment procedures were slightly different in the two cases, the presence of the polysulfidic species and its desorption does not appear to depend strongly on the preparation procedure [7]. Some of the improvement in the diffraction pattern will simply be due to the removal of physisorbed gases, however the majority of these gases were found to be removed by annealing to temperatures of approximately 150°C.

The XPS results discussed above, in addition to previous XPS and XANES studies [5, 8], indicate that the S remaining in the surface region after annealing to approximately 350°C is either bridge-bonded to In in the surface layer, occupies subsurface P positions, or both. If the sulfur is assumed to exist only on the surface, bridge-bonded to In, then the simplest models describing the monolayer system and consistent with the  $1 \times 1$  and  $2 \times 1$  diffraction patterns are shown in Fig. 5. However, these models are inconsistent with our photoemission measurements. We see no electronic states at the Fermi level, and thus the passivated surface is semiconducting. The surface must therefore satisfy the electron counting rule [20, 21], in which all S and P dangling bonds are occupied with two electrons, and all In dangling bonds are unoccupied [18]. Neither of the structures shown in Fig. 5 satisfies this criterion.

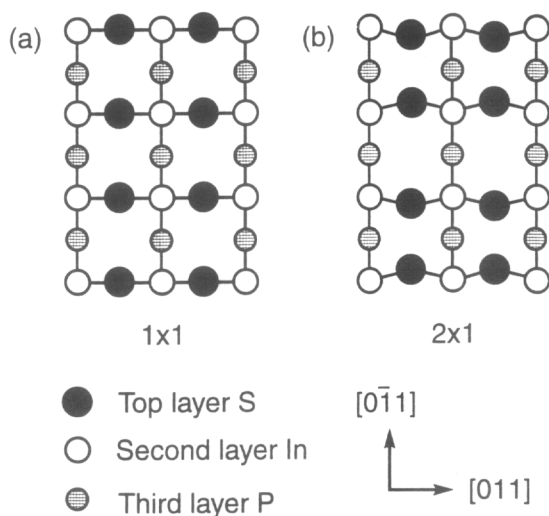


**Fig. 5.** Simple structural models are shown for (a) InP(100)-S  $1 \times 1$  and (b) InP(100)-S  $2 \times 1$ . Neither of these models satisfies electron counting.

In order to satisfy the electron counting rule, one must alter the models shown in Fig. 5 to allow for one or more of the following possibilities: (i) subsurface P or In vacancies, (ii) subsurface S, or (iii) S coverage of less than one monolayer. None of these is inconsistent with the experimental results to date. As noted above, several studies imply the presence of S in subsurface layers [5, 7],

and the P-S exchange is thermodynamically favourable [5]. While several experiments have found that the S coverage is approximately 1 ML [4, 5, 6], it is still not clear how this coverage depends on the details of the preparation and annealing procedures. For example, one study [5] reported a S coverage of 0.5 ML after annealing to 560°C. The RHEED pattern observed for this surface was  $2 \times 1$ . In this case, a surface structure consisting of P-S dimers was proposed, which satisfies electron counting.

The S-passivated InP(100) surface has been shown to contain S in several different chemical environments [5, 6, 7]. As the surface is annealed, the relative proportion of S in these different environments changes. In order to obtain a better understanding of this surface, it is important that a detailed study of the S coverage be performed as a function of preparation procedure and annealing conditions. One of the difficulties associated with this measurement is the need, with techniques such as Auger electron spectroscopy (AES), to know how the S is distributed (surface, subsurface, etc.) before the coverage can be determined. It will probably be necessary, therefore, to correlate the results of several different techniques, such as AES, XPS, low energy ion scattering, and thermal desorption spectroscopy, in order to arrive at consistent results. A knowledge of the S coverage obtained under different conditions, together with further measurements of the S binding sites (performed, for example, with photoelectron diffraction) would provide a solid foundation upon which to base further studies of this surface.

### Acknowledgments

This research was supported by the Natural Sciences and Engineering Research Council of Canada.

### References

1. R. Iyer, R.R. Chang, and D.L. Lile, *Appl. Phys. Lett.* **52**(2), 134 (1988).
2. C.R. Stanley, R.F.C. Farrow, and P.W. Sullivan, in *The Technology and Physics of Molecular Beam Epitaxy*, E.H.C. Parker, (Ed.), Plenum Press, New York (1985), p. 275.
3. G. Eftekhari, *J. Vac. Sci. Technol. B* **12**(6), (1994).
4. Y. Tao, A. Yelon, E. Sacher, Z.H. Lu, and M.J. Graham, *Appl. Phys. Lett.* **60**(21), 2669 (1992).
5. D. Gallet and G. Hollinger, *Appl. Phys. Lett.* **62**(9), 982 (1993).
6. H. Oigawa, J. Fan, Y. Nannichi, H. Sugahara, and M. Oshima, *Jpn. J. Appl. Phys.* **30**(3A), L322 (1991).
7. T. Chassé, H. Peisert, P. Streubel, and R. Szargan, *Surf. Sci.* **331-333**, 343 (1995).
8. Z.H. Lu, M.J. Graham, X.H. Feng, and B.X. Yang, *Appl. Phys. Lett.* **60**(22), 2773 (1992).
9. P.W. Erdman and E.C. Zipf, *Rev. Sci. Instrum.* **53**(2), 225 (1982).
10. N. Babbe, W. Drube, I. Schaefer, and M. Skibowski, *J. Phys. E* **18**, 158 (1985).
11. I. Schaefer, W. Drube, M. Schlueter, and G. Plagemann, *Rev. Sci. Instrum.* **58**(4), 710 (1987).

12. H. Carstensen, R. Claessen, R. Manzke, and M. Skibowski, *Phys. Rev. B* **41**, 9880 (1990).
13. G.W. Anderson, M.C. Hanf, P.R. Norton, Z.H. Lu, and M.J. Graham, *Appl. Phys. Lett.* **65**(2), 171 (1994).
14. X. Hou, G. Dong, X. Ding, and X. Wang, *J. Phys. C* **20**, L121 (1987).
15. J. Woll, Th. Allinger, V. Polyakov, J.A. Schaefer, A. Goldmann, and W. Erfurth, *Surf. Sci.* **315**, 293 (1994).
16. J.E. Ortega and F.J. Himpsel, *Phys. Rev. B* **47**(4), 2130 (1993).
17. S.M. Sze, *Physics of Semiconductor Devices*, John Wiley & Sons, New York (1981).
18. C.E.J. Mitchell, I.G. Hill, A.B. McLean, and Z.H. Lu, to be published in *Applied Surface Science*, proceedings of ICFSI-5, Princeton, N.J. (1995).
19. C.E.J. Mitchell, I.G. Hill, and A.B. McLean, to be published.
20. H.H. Farrell, J.P. Harbison, and L.D. Peterson, *J. Vac. Sci. Technol. B* **5**(5) (1987).
21. M.D. Pashley, *Phys. Rev. B* **40**(15), 10481 (1989).